

Seismic waveform attributes before and after the Loma Prieta earthquake: Scattering change near the earthquake and temporal recovery

Stefan Baisch

Institut für Geophysik, Ruhr-Universität Bochum, Bochum, Germany

Götz H. R. Bokelmann

Department of Geophysics, Stanford University, Stanford, California

Abstract. During 1987-1995 several clusters of nearly identical seismic events (multiplets) occurred near the Loma Prieta source region. These multiplets allow us to investigate and demonstrate spatial and temporal changes in seismic wave character associated with the 1989 Loma Prieta main shock. For seismogram pairs we use a moving window technique to compute coherencies depending on lapse time and frequency. Post-Loma Prieta events have reduced coherencies with pre-Loma Prieta events in a spatially limited region close to the Loma Prieta hypocenter, while other paths remain nearly unaffected. These changes gradually recover within a time interval of 5 years after the Loma Prieta earthquake. A possible explanation for the time dependence is coseismically opened cracks which cause scattering increase for wavefields after the Loma Prieta event. Postseismic relaxation processes such as crack healing, fluid diffusion, or after deformations lead to progressive closure of these cracks with time after the main shock. Thus the scattering properties of the local crust approach the pre-main shock state.

1. Introduction

Aside from the 1906 San Francisco earthquake, the $M=6.9$ Loma Prieta quake was the largest and most damaging quake to strike an American urban area in this century [Holzer, 1999]. Although disastrous from a hazard point of view, Loma Prieta provides an excellent opportunity for improving our understanding of all aspects of large earthquakes since it occurred in a densely instrumented region. In the past 10 years many studies of Loma Prieta have already given a rather detailed picture of the earthquake [e.g., Spudich, 1996; Reasenber, 1997; Simpson, 1994]. Nevertheless, there are important open questions related to rheological properties of the fault zone and the nature of after event deformation. These questions may in principle be addressed by studying seismic waves, which carry information about the source region and the medium they pass through. Especially interesting is the study of changes in the character of seismic waves with time (months to years) since these give direct clues to changes of material behaviour with time. In the past, researchers attempted

to demonstrate such changes by studying attenuation (coda Q) and seismic wave velocities.

For this purpose, a number of active experiments were conducted to resolve stress induced velocity changes [e.g., Eisler, 1967, 1969; Aki *et al.*, 1970; DeFazio *et al.*, 1973] or to monitor temporal changes of the velocity field associated with big earthquakes [e.g., Karageorgi *et al.*, 1992; Li *et al.*, 1998]. Besides repeated active experiments which are too weak to illuminate the whole crust, researchers considered earthquake sources which sample the crust at different times. A fundamental problem with this approach comes from the lack in the repeatability of the source. This led to controversies as to whether or not reported velocity changes are real [e.g., Wesson *et al.*, 1977]. Prominent examples are studies of precursory phenomena in P and S wave velocities [e.g., Kanamori and Fuis, 1976]. Other groups inspected coda attenuation for changes with time. While Aki and Chouet [1975] suggest that coda Q shows time variations due to subsurface medium changes, other studies indicated that coda Q may not be a stable estimator of attenuation [see Sato, 1988; Got *et al.*, 1990; Got and Fréchet, 1993].

More recently, a number of studies did not find changes in coda Q attenuation but were able to give upper bounds [Hellweg *et al.*, 1995; Antolik *et al.*, 1996; Aster

Copyright 2001 by the American Geophysical Union.

Paper number 2001JB000151.
0148-0227/01/2001JB000151\$09.00

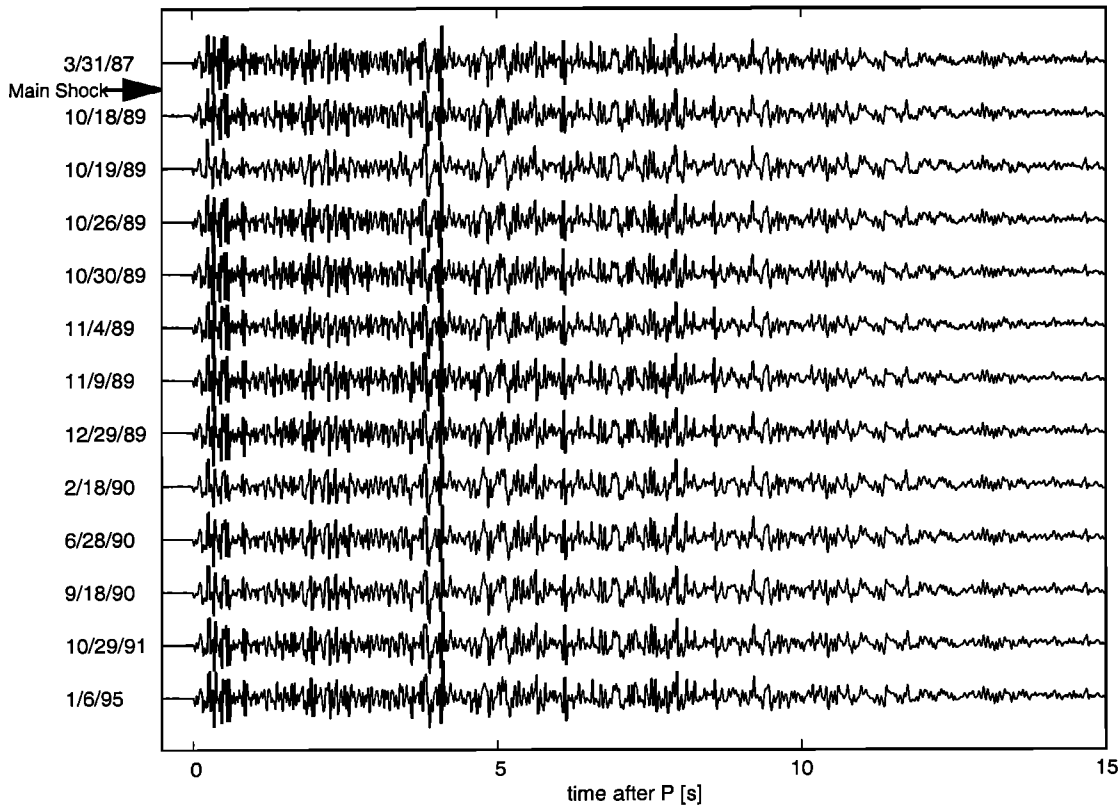


Figure 1. Waveforms of multiplet p2 recorded at station HFP southeast of the rupture zone (Figure 3). Event dates are marked on the left. Data are aligned to the P onset. Note the high waveform similarity throughout the entire 15 s time window.

et al., 1996]. For the Loma Prieta after shocks an upper bound was given as 5% [Beroza *et al.*, 1995].

The existence of temporal variations in a crustal setting is clearly controversial. That is quite different in the smaller-scale problem of reservoir geophysics, where the variation of properties with time is well established and of considerable practical importance [Jack, 1998]. In the whole-crust setting, there is a need for showing unambiguous evidence for temporal changes in seismic properties. That is the focus of the current paper, which presents examples of subsurface changes after Loma Prieta. These are documented in waveform changes of “similar” events. The technique we use is based on waveform similarities rather than the coda Q technique because we find that the latter is subject to a number of rather restrictive assumptions, which are not strictly necessary for showing the existence of temporal changes.

The critical ingredient of our technique is the use of sets of similar events [e.g., Aster *et al.*, 1990], which we will call seismic multiplets. This allows good control of source effects. We perform a multi station analysis which clearly restricts the observed similarity decrease to a spatially limited region, thus showing the robustness of the technique against data contaminations such as potential source variations. From successive combination of repeating earthquakes sampling the crust at

different times we can study the temporal evolution of waveform similarity, i.e., its gradual recovery after the Loma Prieta earthquake.

2. Data

A common feature of seismicity along major faults is the occurrence of spatially tightly clustered microearthquakes. These clusters often represent stress release at the same asperity, or stress concentration, along a fault surface [Geller and Mueller, 1980]. If all member events of such clusters are approximately collocated and have the same source radiation pattern, the generated waveforms are nearly identical for the entire cluster. In practice, however, each event in a cluster has its own source volume, and it is difficult to decide whether these volumes are perfectly collocated. Following Geller and Mueller [1980], we take the $\lambda/4$ criterion, i.e., all events must be separated by less than a quarter wavelength, to define a cluster that we will call a seismic multiplet hereinafter.

At the southern end of the Loma Prieta rupture zone and in the vicinity of the Morgan Hill epicenter on the Calaveras Fault, several multiplets with interevent separation of not more than a few tens of meters have been identified (D. Schaff, personal communication, 1999). These multiplets consist of up to 20 events which pro-

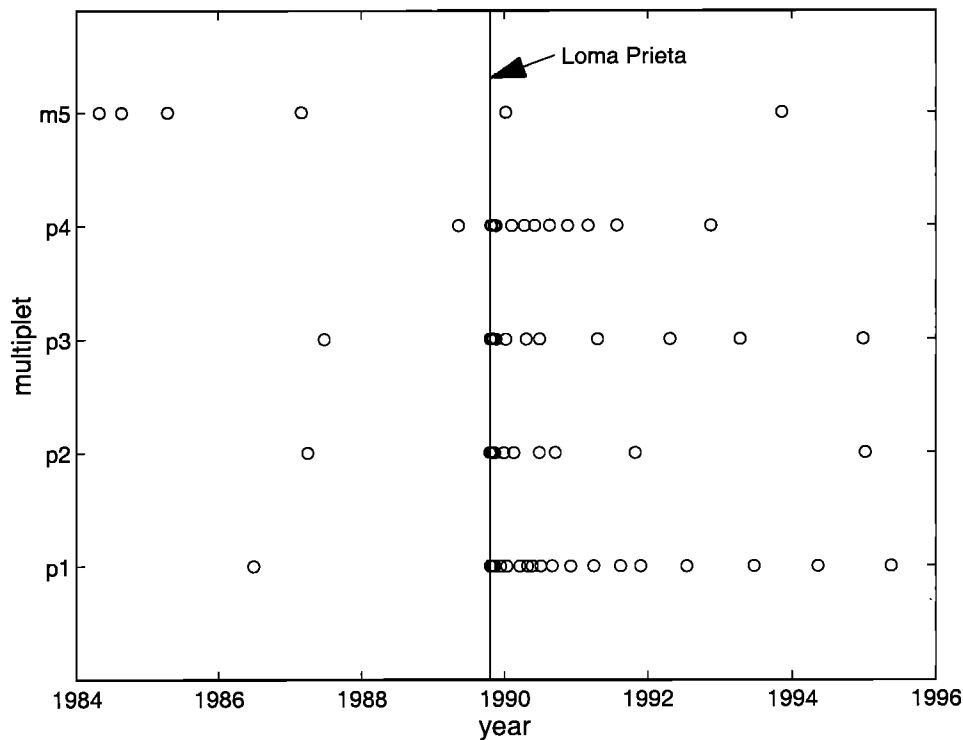


Figure 2. Time lines of five multiplets sampling the Loma Prieta earthquake. Event times are shown by circles; the vertical line indicates the time of the Loma Prieta earthquake. Multiplets p1-p4 are located at the southern end of the Loma Prieta rupture zone, and multiplet m5 is located on the Calaveras Fault (marked by arrows in Figure 3).

duce nearly identical waveforms. Figure 1 shows an example of the waveforms of multiplet p2 recorded at station HFP. The waveforms are raw data as distributed by the Northern California Earthquake Data Center (NCEDC) [Neuhauser *et al.*, 1994].

The five multiplets we used for our analysis sample the Loma Prieta earthquake in time; that is, at least one of their events occurred before the main shock, and several event members occurred after the main shock (Figure 2 and Table 1). We will refer to these events as preshock and aftershocks, respectively.

In this paper we focus on the 13-element multiplet p2. In order to keep a fixed station network for our investigations we chose the subset of the Northern California Seismic Network (NCSN) stations for which most of the recordings pass our selection criteria (described below). The station net used in our analysis is defined on basis of the station coverage of multiplet p2 which is better than for the other multiplets. We aimed to include as many stations as possible and searched the entire NCSN for stations that satisfy our selection criteria. In addition to an excellent signal-to-noise ratio (SNR) we required that no alterations of the instrumentation have been undertaken between the preshock and the aftershocks. This criterion excludes stations which have been converted from analog to digital as well as those for which the gain ranging has been changed. We did not use the data from a number of available broadband

stations to avoid complications from differing instrument types. The short-period stations (Figure 3) are equipped with Mark L4-C instruments and were operated at a sampling frequency of 100 Hz.

3. Spatial Variations in Doublet Similarity

A simple approach which clearly demonstrates changes of crustal properties near the Loma Prieta rupture zone is based on seismogram cross correlations in the time domain. Figure 4 shows cross-correlation coefficients between the preshock and the first aftershock of multiplet p2 (see Table 1). At each station, cross correlations are computed in a 15 s time window starting at the *P* onset. The resulting pattern is clearly divided into two regions. Stations to the northwest, for which the direct waves traveled mainly through the rupture zone of the Loma Prieta earthquake, systematically show reduced cross-correlation values, whereas stations in other azimuths show correlation values above 0.9. Basically, the same pattern is reproduced using preshock-aftershock combinations of the multiplets p1, p3, and p4, which are located close to p2 (Figure 3). In principle, several factors can explain locally reduced cross-correlation values. Most critical are changes in source parameters, but these can be excluded by the pattern resulting from the Calaveras Fault multiplet.

Table 1. Origin Times, Northern California Seismic Network Locations, and Coda Magnitudes of Events Used in This Study ^a

Multiplet	Number	Year	Month	Day	Time, LT	Latitude, °N	Longitude, °E	Depth	Magnitude
p1	1	1986	6	28	064304	36.94	-121.68	10.6	1.1
p1	2	1989	10	20	171953	36.94	-121.68	10.9	1.2
p1	3	1989	10	28	112337	36.95	-121.68	10.9	1.0
p1	4	1989	11	5	041144	36.94	-121.68	10.3	1.1
p1	5	1989	11	12	124322	36.94	-121.68	10.8	1.3
p1	(6)	1989	12	12	215443	36.94	-121.68	10.6	1.4
p1	(7)	1990	1	13	003411	36.95	-121.68	10.9	1.5
p1	8	1990	3	20	195755	36.94	-121.68	10.5	1.3
p1	9	1990	4	28	070941	36.94	-121.68	10.4	1.1
p1	10	1990	5	23	152354	36.94	-121.68	10.7	1.1
p1	11	1990	7	5	023007	36.94	-121.68	10.2	1.2
p1	12	1990	9	2	190742	36.94	-121.69	10.8	1.2
p1	(13)	1990	12	6	205752	36.94	-121.68	11.4	1.5
p1	14	1991	4	2	060214	36.94	-121.68	11.1	1.3
p1	15	1991	8	16	201638	36.95	-121.68	10.3	1.1
p1	16	1991	11	25	020150	36.94	-121.68	10.4	0.9
p1	(17)	1992	7	16	050228	36.94	-121.68	11.0	1.4
p1	18	1993	6	22	101107	36.94	-121.68	10.8	0.9
p1	19	1994	5	12	020247	36.94	-121.68	11.1	1.2
p1	20	1995	5	17	041852	36.94	-121.69	10.8	1.1
p2	1	1987	3	31	061920	36.94	-121.68	10.2	1.8
p2	2	1989	10	18	231153	36.94	-121.68	10.0	1.6
p2	3	1989	10	19	173631	36.94	-121.68	9.9	1.5
p2	4	1989	10	26	024756	36.94	-121.68	10.1	1.8
p2	5	1989	10	30	214955	36.94	-121.68	10.1	1.6
p2	6	1989	11	4	021207	36.94	-121.68	9.7	1.4
p2	7	1989	11	9	073334	36.94	-121.68	10.2	1.5
p2	8	1989	12	29	213458	36.94	-121.68	10.4	1.9
p2	9	1990	2	18	025056	36.94	-121.68	10.1	1.8
p2	10	1990	6	28	072811	36.94	-121.68	10.2	1.9
p2	11	1990	9	18	010310	36.94	-121.68	10.1	1.7
p2	12	1991	10	29	233158	36.94	-121.68	10.1	1.9
p2	13	1995	1	6	162811	36.94	-121.68	9.6	2.0
p3	1	1987	6	22	195509	36.94	-121.68	10.2	1.7
p3	2	1989	10	19	152056	36.94	-121.68	10.5	1.8
p3	3	1989	10	21	101338	36.94	-121.68	10.4	2.0
p3	4	1989	10	23	120621	36.94	-121.68	9.7	1.7
p3	5	1989	10	26	024334	36.94	-121.68	9.8	1.7
p3	6	1989	11	4	224941	36.94	-121.68	9.8	1.5
p3	7	1989	11	18	180805	36.94	-121.68	10.1	1.8
p3	8	1990	1	7	210053	36.94	-121.68	10.4	1.8
p3	9	1990	4	21	144455	36.94	-121.68	10.4	2.1
p3	10	1990	6	28	073020	36.94	-121.68	9.9	1.7
p3	11	1991	4	20	235911	36.94	-121.68	10.5	1.6
p3	12	1992	4	21	091729	36.94	-121.68	10.4	1.8
p3	13	1993	4	11	064610	36.94	-121.68	10.6	1.7
p3	14	1994	12	25	224816	36.94	-121.68	10.4	1.7
p4	1	1989	5	11	005704	36.94	-121.68	11.8	1.6
p4	(2)	1989	10	22	214831	36.94	-121.68	12.0	2.3
p4	(3)	1989	10	24	182533	36.94	-121.68	11.8	2.1
p4	(4)	1989	10	28	234545	36.94	-121.68	11.9	1.0
p4	5	1989	11	8	010605	36.94	-121.68	11.9	1.5
p4	(6)	1989	11	12	195649	36.94	-121.68	11.3	1.0
p4	7	1989	11	19	211405	36.94	-121.68	11.8	1.5
p4	8	1990	2	6	005025	36.94	-121.68	11.8	1.6
p4	9	1990	4	12	053555	36.94	-121.68	11.9	1.8
p4	(10)	1990	6	4	200618	36.94	-121.68	11.7	1.3
p4	11	1990	8	19	193306	36.94	-121.68	12.3	1.5
p4	(12)	1990	11	19	064803	36.94	-121.68	12.1	0.9
p4	13	1991	3	4	193206	36.94	-121.68	12.2	1.8
p4	(14)	1991	7	28	081236	36.94	-121.68	12.6	1.0
p4	15	1992	11	14	060854	36.94	-121.68	12.5	1.5
m5	(1)	1984	4	25	005201	37.24	-121.63	4.8	2.6

Table 1. (continued)

Multiplet	Number	Year	Month	Day	Time, LT	Latitude, °N	Longitude, °E	Depth	Magnitude// height
m5	2	1984	8	18	115428	37.24	-121.63	4.9	2.3
m5	3	1985	4	11	103459	37.24	-121.63	5.2	2.3
m5	4	1987	2	26	144436	37.24	-121.63	5.5	2.3
m5	5	1990	1	7	150309	37.24	-121.63	5.3	2.2
m5	6	1993	11	9	191734	37.24	-121.63	5.1	2.2

^a We use only those events which are similar in magnitude. All events not used for our analysis but used by *Beroza et al.* [1997], *Schaff et al.* [1998], and D. Schaff and G. C. Beroza (manuscript in preparation, 2000) are shown in parentheses.

As will be shown below, a similarity decrease can be observed for the m5 multiplet (Figure 3) only for stations close to the Loma Prieta rupture zone. From the limited spatial pattern combined with the redundant observations we can also rule out contamination effects such as local changes of the background noise level or changes of water saturation due to rainfall. Thus we conclude that the decrease of waveform similarity is caused by local changes of crustal properties.

To study the nature and localization of these changes in more detail, we applied a moving-window analysis of seismogram similarity implemented in the frequency domain. The analog of the cross correlation in the time domain is the coherency in the frequency domain, which

can be defined as [e.g., *Jenkins and Watts*, 1968, chap. 8 and 9]

$$C(\nu) = \frac{|\gamma_{xy}(\nu)|}{\sqrt{\gamma_{xx}(\nu)\gamma_{yy}(\nu)}} \quad (1)$$

Here $\gamma_{xy}(\nu)$ denotes the smoothed cross spectrum of seismograms $x(t)$, say the preshock, and $y(t)$, say one of the aftershocks, and $\gamma_{xx}(\nu)$ denotes the smoothed autospectrum of $x(t)$. A proper treatment of confidence intervals for the coherency is presented in Appendix A.

We computed coherencies in 2.56 s time windows, which we shift by steps of 1.28 s. As a smoothing function we chose a five-point spectral operator, defined by the Fourier transform of a Tukey window. For this

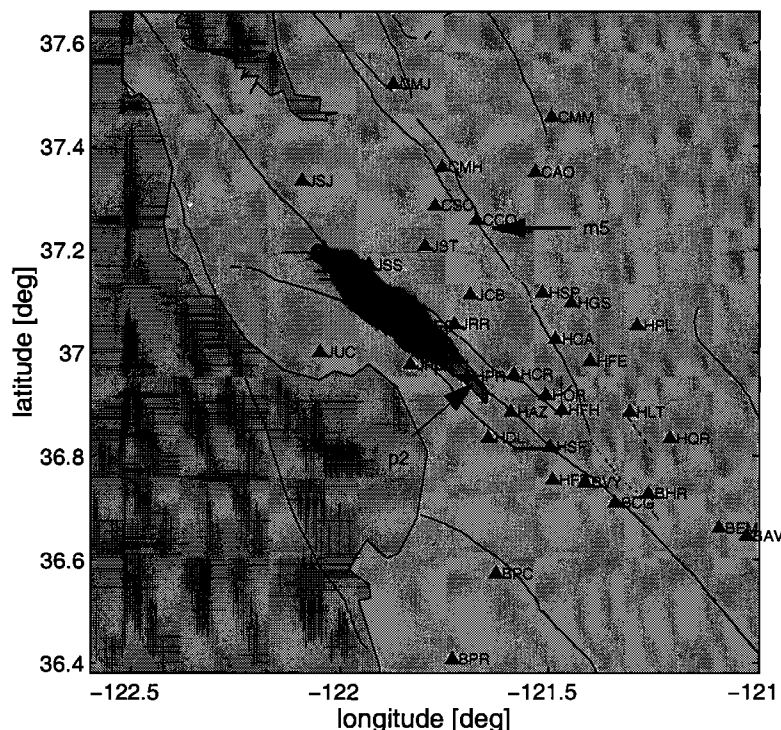


Figure 3. Map of the San Francisco Bay area showing the Loma Prieta rupture zone (shaded area) as defined by the aftershock distribution (D. Schaff, personal communication, 1999). Two multiplets used in this study are located near the southern end of the rupture zone (p2) and on the Calaveras Fault (m5). California Seismic Network stations used in this study are shown by triangles. Solid lines show surface traces of mapped faults.

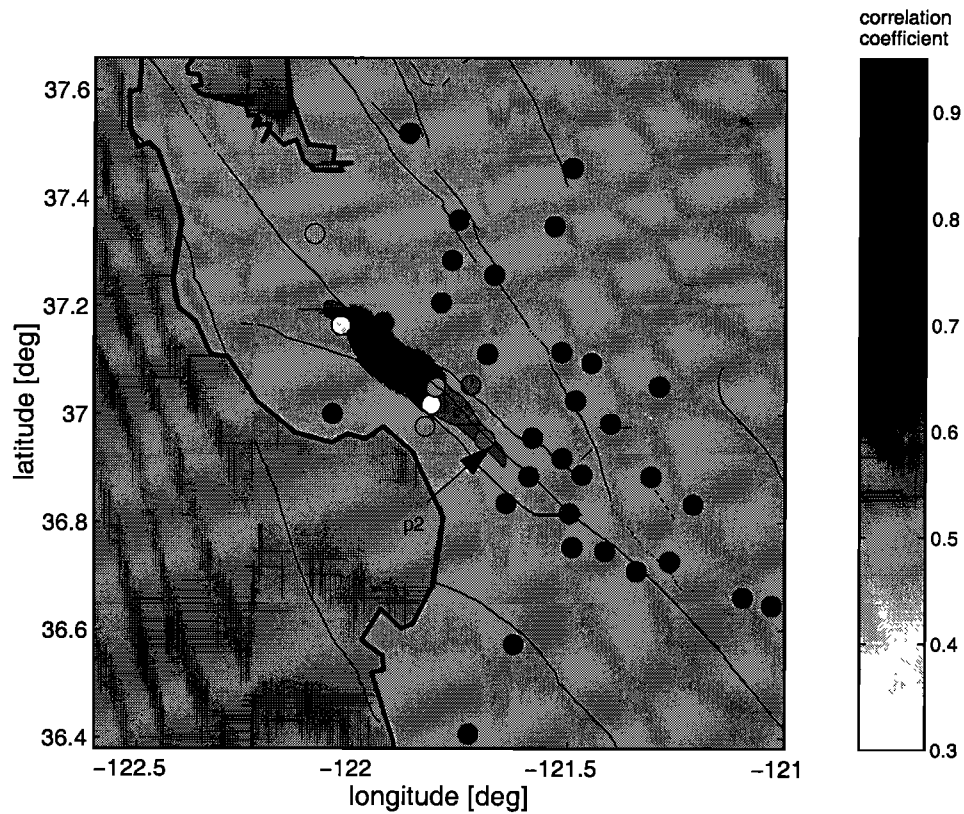


Figure 4. Seismogram cross correlations between the preshock and the first aftershock of multiplet p2 (Table 1). Cross-correlation coefficients are computed using the 15 s time window starting at the *P* onset. Note that owing to the Loma Prieta earthquake, seismogram similarities are strongly decreased in vicinity of the rupture zone, while they vary only little at most other stations.

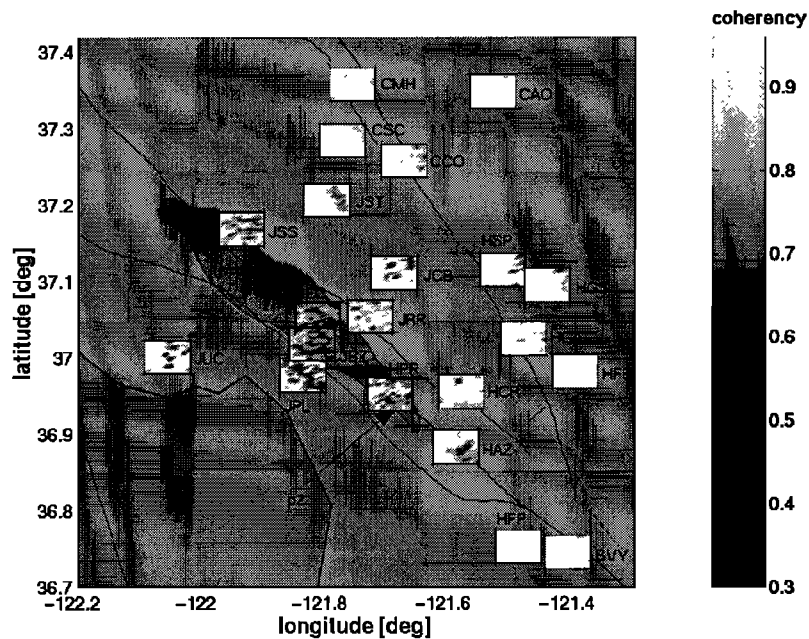


Figure 5. Seismogram coherencies between the preshock and the first aftershock of multiplet p2. At each station coherencies are shown as a function of lapse time (*x* axis) and frequency (*y* axis). The time range is 11.52 s starting 1.28 s after *P*. The frequency range is 2-10 Hz. See text for more details.

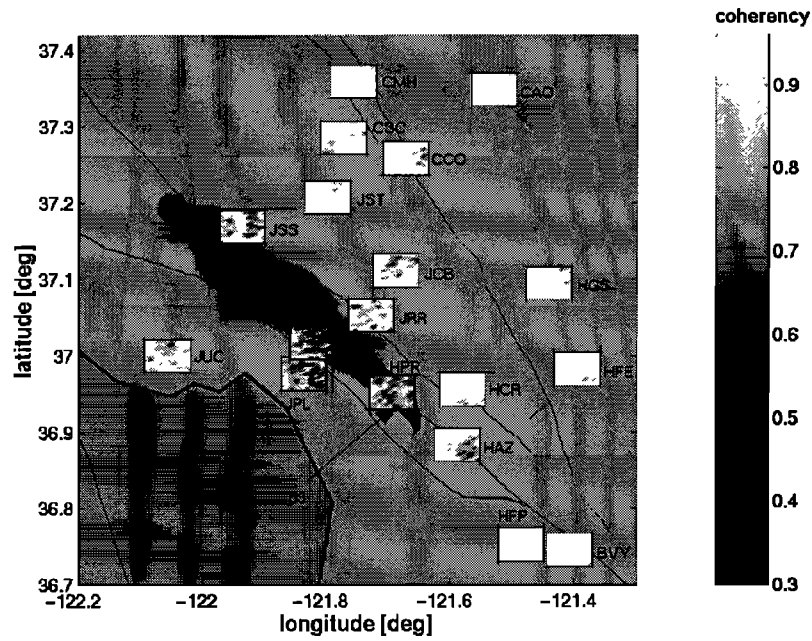


Figure 6. Seismogram coherencies between the preshock and the first aftershock of multiplet p3. Display is as in Figure 5.

smoothing operator the lowest limit to the coherency that may be determined is ~ 0.06 . In Figure 5, coherencies for the same data example as in Figure 4 are displayed. At each station, coherencies are shown as a function of lapse time (x axis) and frequency (y axis). The frequency range is restricted to 2-10 Hz to avoid effects due to changes in event magnitude (see Table 1) at higher frequencies and to reduce possible contaminations from noise at lower frequencies. We display only

the subset of stations used in Figure 4, which have a reasonable coverage of the events in the multiplet. This will be especially important for the temporal aspect addressed in section 4. As expected from Figure 4, low coherency values mainly exist at stations northwest of the multiplet epicenter. At some surrounding stations, minor decreases of coherency of single seismogram phases are resolved which were previously masked by the long time window used for calculating the cross correlations.

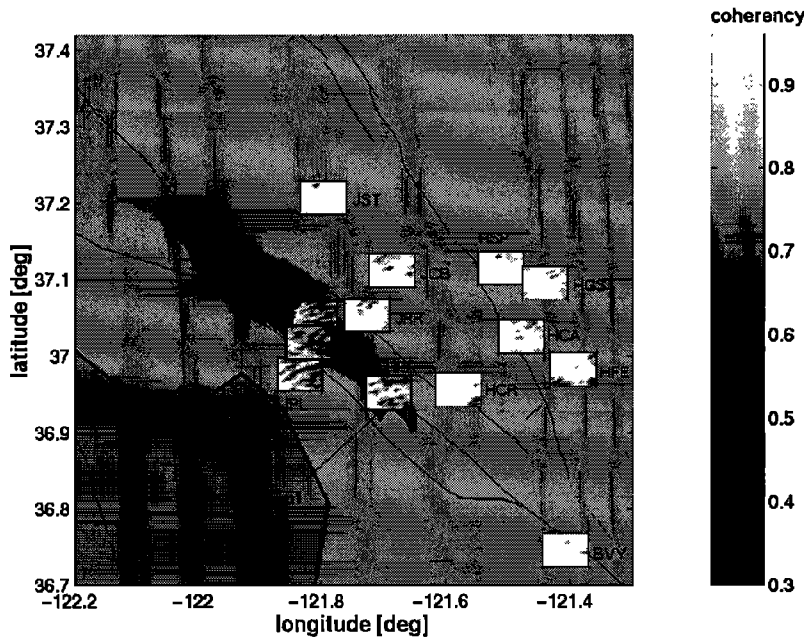


Figure 7. Seismogram coherencies between the preshock and the first aftershock of multiplet p1. Display is as in Figure 5.

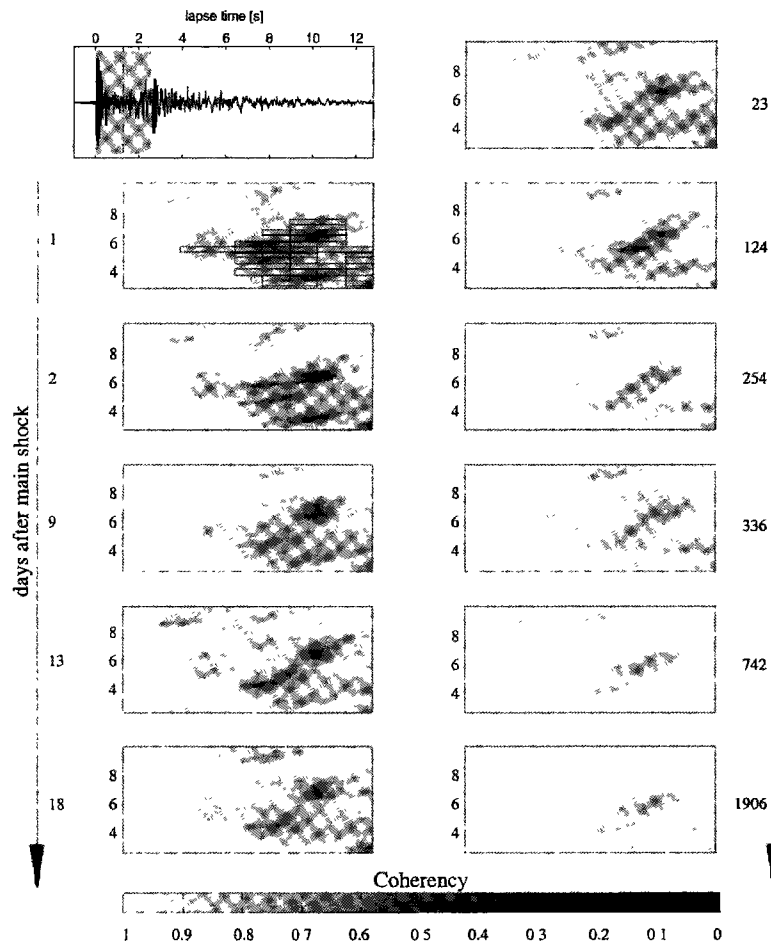


Figure 10. Coherencies for all preshock-aftershock combinations at station HAZ. Top left shows the waveform of the preshock. The time window used for the calculation of the coherencies is indicated by the shaded area. Coherencies between the preshock and aftershocks are shown depending on lapse time (x axis) and frequency (y axis), following the event time of the aftershocks in days after the Loma Prieta main shock, which is indicated along the arrows. Note that patches of anomalous low coherencies (marked by the boxes in the plot for 1 day after main shock) progressively decrease with increasing time after Loma Prieta.

already seem to have sampled the scattering region and transferred information about that region into their coda waves.

An almost identical coherency pattern to that of Figure 5 is observed for multiplet p3 (Figure 6), which is located only a few hundred meters away from multiplet p2 (D. Schaff, personal communication, 1999). These independent observations demonstrate that reduced coherencies indeed are due to subsurface changes and do not reflect seismogram contaminations (note the different event times of the preshock and aftershocks of these two multiplets; see Table 1). Multiplets p1 and p4 also produce similar coherency patterns (Figures 7 and 8), although lower magnitudes in multiplet p1 cause additional coherency decrease at more distant stations (e.g., HFE) owing to a lower signal-to-noise ratio.

The coherency pattern of the Calaveras Fault doublet shown in Figure 9 is also compatible with the assumed location of scatterer. Comparing Figure 5 and 9, we

note that the coherency decrease at JBZ viewed from the Calaveras Fault starts ~ 1 s later in the seismogram than viewed from the San Andreas Fault. This might be an indication that the scatterer is not located in the immediate vicinity of station JBZ, in which case the onset of scattered phases would be azimuthally independent.

4. Temporal Variations of Seismogram Similarities

In section 3 we focused on localizing medium changes which have been generated in the “Loma Prieta time interval” between the preshock and the first aftershock of the multiplets. Now we study the temporal evolution of these scatterers by successively comparing the preshock to all aftershocks of multiplet p2 (listed in Table 1). Figure 10 shows these combinations at station HAZ. As already demonstrated in Figure 5, a strong coherency decrease occurred for the combination of the preshock

with the first aftershock. This decrease is confined to frequencies below 8 Hz and sets in at lapse times > 6 s. For combinations with subsequent aftershocks the same lapse time-frequency range (TFR) is affected, but coherencies within this TFR gradually increase with time after Loma Prieta. The only time interval in which the medium experienced strong changes is one which contains the Loma Prieta event (between the preshock and first aftershock). The faster recovery within the first days after the main shock demonstrates that the coherency reduction is indeed due to the Loma Prieta event.

In order to quantify the recovery process we applied a simple threshold test to the coherencies of the preshock and first aftershock (Figure 10, left, second panel). We defined the TFR where coherencies dropped below a value of 0.75. This marked region is held constant and applied to the subsequent aftershocks (following panels in Figure 10). Further, we defined $\tilde{C} = 1 - \bar{C}$, where $\bar{C}(t)$ denotes the mean coherency in the marked TFR. In Figure 11, \tilde{C} is plotted against event time of the aftershocks on a semilogarithmic scale. This type of presentation provides a compact way of visualizing the recovery process. As indicated by the solid line, the coherency increase approximately follows a power law dependence. Also shown in Figure 11 is an estimate of the entirely recovered coherency obtained as the \tilde{C} value

of the last two aftershocks. This value is still smaller than for the combination of the preshock with the last aftershock, indicating that the recovery is not complete within the observation time of ~ 5.25 years.

In the next step we applied the same averaging procedure to the other stations used in Figures 5-9. To ensure a reasonable temporal coverage of events at each station, we further restricted our analysis to those stations where a minimum number of multiplet events are available according to our selection criteria. For multiplet p2 we chose a minimum number of 10 events. Since the threshold test works only at stations where coherency values exist below the threshold, we switched the threshold to a higher value of 0.985 at those stations where < 10 TFR data points exhibit coherency values below 0.75. The higher threshold value is chosen such that a similar distribution of affected TFR data points exists for both station sets. Figure 12 maps the resulting time signals for multiplet p2. Although there is more scatter in the data at some stations, a similar recovery relation exists at all stations near the rupture zone. Even at more distant stations, especially in the eastern part, a slight but systematic coherency increase with time can be observed, suggesting that backscattered phases are still measurable at these stations. In contrast, at the northern stations CMH, CSC, and CAO, temporal changes of coherencies obviously

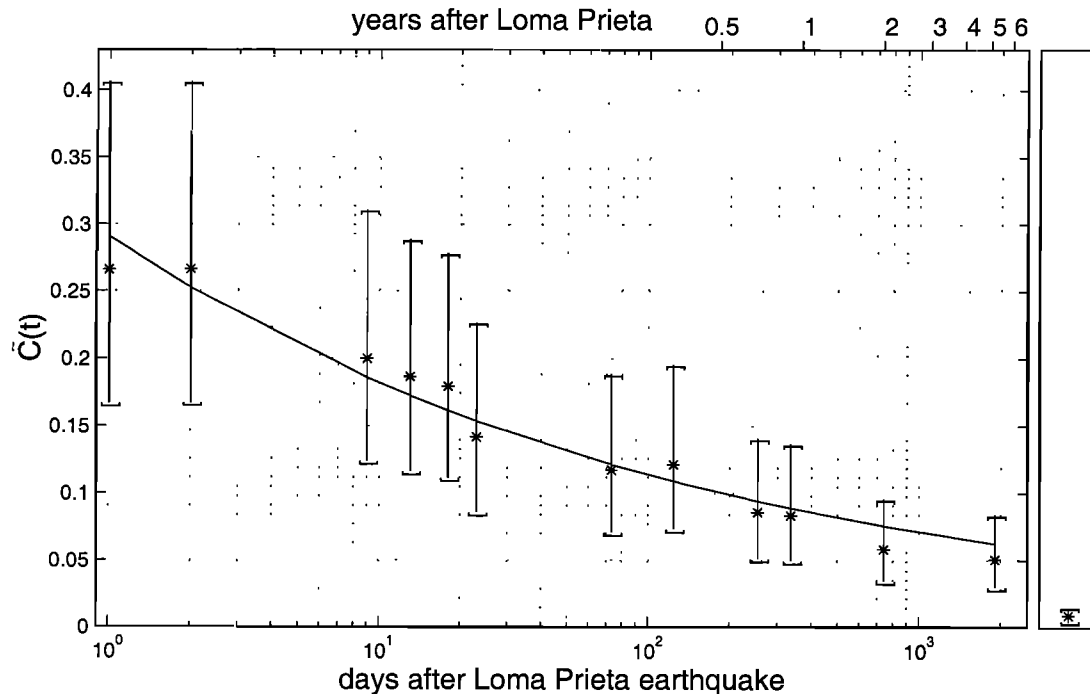


Figure 11. Recovery of waveform similarity for p2 as observed in a temporal increase of coherencies at HAZ. Asterisks denote $\tilde{C}(t) = 1 - \bar{C}(t)$, where $\bar{C}(t)$ is the mean coherency in the anomalous region of Figure 10. Time is shown with respect to the Loma Prieta earthquake (semilogarithmic scale). Error bars indicate 95% confidence intervals (see Appendix A for details). The solid line shows a fit to a power law dependence of the form $\tilde{C}(t) = a t^{-p}$. The panel on the right shows the \tilde{C} value for the last two events of multiplet p2 as an estimate of the entirely recovered coherency.

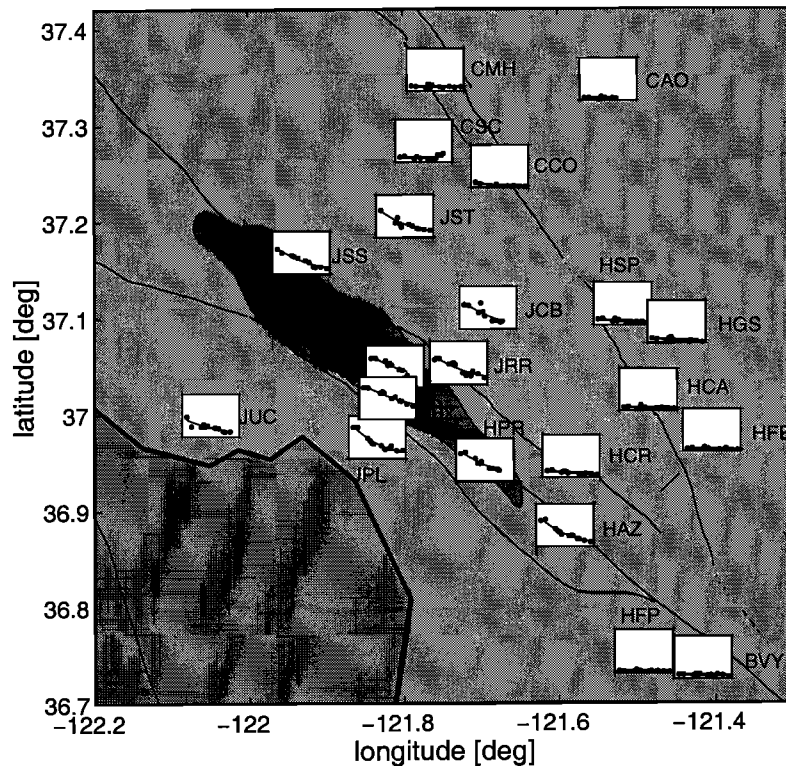


Figure 12. Coherency recovery at all stations for multiplet p2. Station boxes show mean coherency depending on time after Loma Prieta. For these boxes, scaling on the x axis is the same as in Figure 11. On the y axis the range between 0 and 0.5 is shown. Solid line indicates the best fit to a power law curve.

are caused by noise effects since no systematic pattern is present.

In general, stations at greater distance to the assumed scatterer location show smaller temporal variations of the coherencies. We interpret this as an effect of the geometrical attenuation of the scattered phases making them lower in amplitude compared to the near-station-generated coda waves at greater distances. The same argument can also explain why the recovery process at the central station JBZ seems to be less complete within the observation time compared to stations at intermediate distances (JUC, JSS, JST, HCR, and HAZ). A remarkably similar recovery signal is observed for multiplet p3 (Figure 13). To obtain a similar station subset as in Figure 12, we chose a minimum number of nine events required at each station. Except for station JST the recovery signals in Figures 12 and 13 match fairly well. For multiplet p2 (Figure 12) the recovery signal at JST is steeper than for multiplet p3 (Figure 13). This might be caused by slight differences of the propagation path between the p2 and p3 events and/or differences in frequency content such that the p2 and p3 waveforms sample the anomalous region in a different way.

We do not show the recovery signals for multiplets p1 and p4 where a reasonable number of events is only available for a few stations. At these stations the recovery signal is comparable to that in Figures 12 and 13.

Compared to the other multiplets, the signal-to-noise ratio of multiplet p1 events (Table 1) is poor, and we had to exclude many noisy recordings of this multiplet in advance.

5. Discussion

We find a strong coherency decrease associated with the Loma Prieta earthquake which gradually recovers with the years after the event. Different from this data-driven approach, *Beroza et al.* [1995] applied a formal coda Q technique and found stable coda Q values (upper bound of 5%). However, the coda Q technique is commonly (and necessarily) stabilized by weighting functions which reject data of low coherency [*Got et al.*, 1990]. This suppresses exactly those data which in the present study show the temporal variations.

Using the same multiplet data sets, *Beroza et al.* [1997] and D. Schaff and G. C. Beroza (manuscript in preparation, 2000) find changes in seismic wave velocities which show a similar recovery signal to that reported here. The spatial pattern of delayed seismogram phases as well as the onset of these phases at each individual station resemble the pattern of reduced coherencies observed in this study, thus indicating that both methods reflect the same crustal changes. The critical difference between the two approaches comes from the

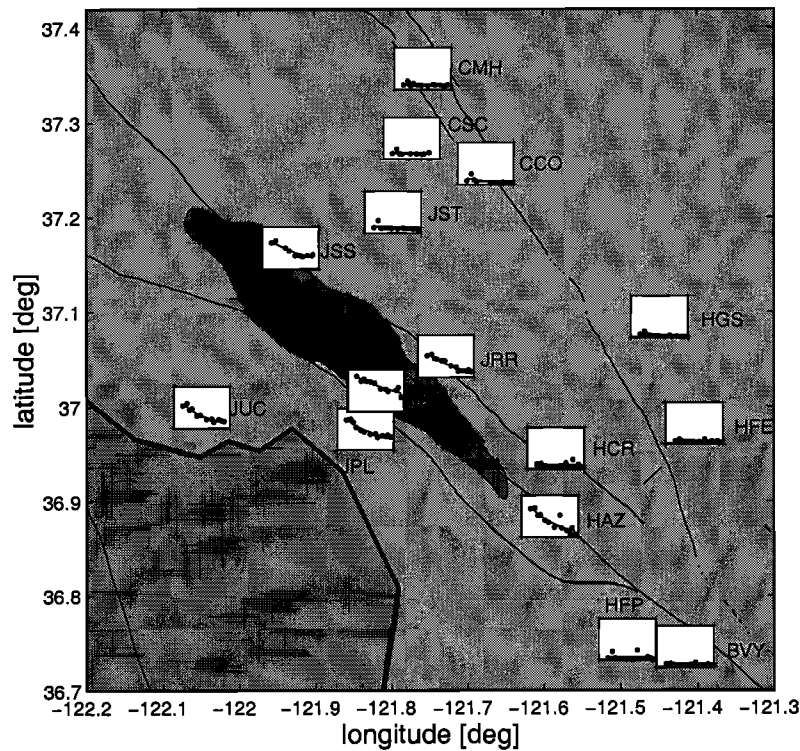


Figure 13. Coherency recovery at all stations for multiplet p3. Display is as in Figure 12.

fact that velocity delays can be observed in the transmitted wavefields of crustal changes only. Therefore it is difficult to interpret the present observations as pure delay effects. For instance, consider station HAZ in Figure 5. Explaining the coherency pattern at this station in terms of pure delay effects would require a seismogram phase which travels from the multiplet hypocenter to the anomalous region (which obviously is located northwest to the multiplet hypocenter), samples that region (where the phase is delayed), and is reflected back to station HAZ. From kinematic arguments the phase cannot travel much farther than station JBZ to the northwest, even when assuming single scattering. Thus it seems more likely that the anomalous region itself acts as a reflector, and we suggest that our observations are caused by additionally scattered phases, rather than by delayed phases. The coherency analysis presented here can be regarded as a tool for identifying additional phases in two otherwise identical seismograms without invoking a physical model of the scattering processes. Although the coherency itself is a statistical property which cannot be related easily to physical parameters, coherency-based techniques proved to be useful for phase identification [e.g., *Leśniak and Nitsuma, 1998*]. By kinematic arguments, these observations can be related to scattering changes in the vicinity of station JBZ. In principle, the coherency provides no information whether the postseismic or the preseismic wave fields experienced enhanced scattering, but it seems more plausible that scattering was enhanced during the rupture process rather than reduced.

Figures 5 and 9 may indicate that the scatterer is not located in the immediate vicinity of station JBZ. Then the scatterer location would have either a horizontal or a vertical offset to station JBZ. From the coherencies alone it appears difficult to distinguish between a shallow or a deep location, but in the latter case the scatterer might directly coincide with the region of highest deformation during the Loma Prieta earthquake (Figure 14). Borehole observations at depth suggest that temporal variations in the deeper crust exist [*Bokelmann and Harjes, 2000*]. They are not necessarily confined to the near-surface region. However, applying a source array analysis to similar events in the Loma Prieta region, *Dodge and Beroza [1997]* find that most of the coda waves leave the source in direction of the recording station indicating that the coda consists primarily of waves scattered near the stations. Thus they suggest that coseismic velocity decrease associated with the Loma Prieta earthquake as observed by *Ellsworth et al. [1992]* occurred in the shallow crust, near the stations. Nevertheless, to explain the coherency patterns in Figures 5-9 phases are required which leave the source in different directions. Therefore the line of argument of *Dodge and Beroza [1997]* does not apply to the observations presented here, and we think that at this point, neither of the observations can be used to distinguish between a shallow or a deep location.

To relate our observations to a physical model, we suggest that coseismic deformation leads to crack opening either by local concentrations of shear stress (coseismic dilatancy) or by elevated pore fluid pressure.

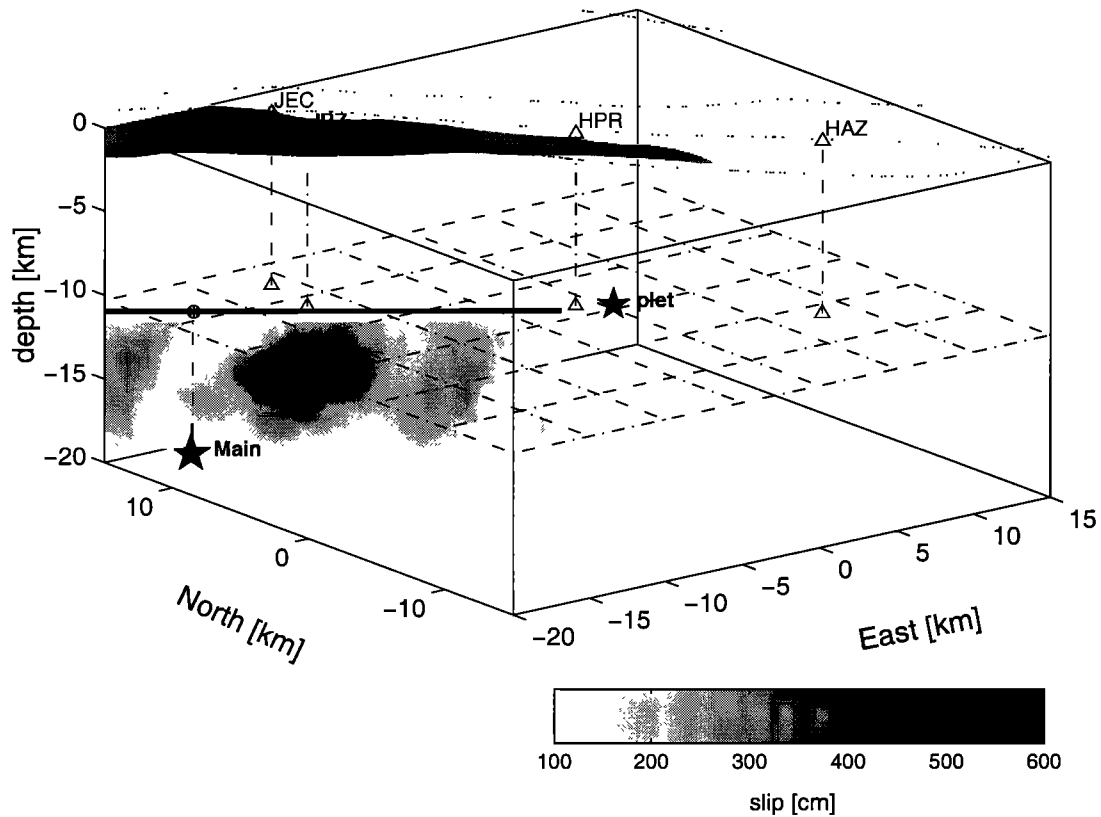


Figure 14. Diagram showing the southern part of the Loma Prieta slip model of Beroza [1996]. Stars denote the main shock and the multiplet p2 hypocenter, respectively. Some station locations and their projection into the multiplet depth (gridded plane) are shown. Note that JBZ is located just above the high-slip area where slip exceeded 5 m.

In the postseismic wave fields these cracks are seen as additional seismic reflectors [e.g., *Nur and Walder, 1992*]. Immediately after the earthquake, relaxational processes start and cause the cracks to close again. Possible candidates for such processes are crack healing [*Smith and Evans, 1984*], successive decrease of pore fluid pressure by diffusion [*Booker, 1974*], and postseismic deformations lowering shear stress concentrations [*Schaff et al., 1998*]. The temporal evolution of all these processes follows a typical power law dependence compatible with our observations. Anomalous postseismic deformations after Loma Prieta are observed in GPS measurements [*Savage et al., 1994*; *Bürgmann et al., 1997*; *Segall et al., 2000*] and exhibit a compressional component normal to the San Andreas Fault. These deformations seem to occur in the brittle part of the crust and might reflect the postseismic response to coseismic dilatancy [*Savage et al., 1994*]. However, it is difficult to directly compare the surface deformations with the healing signal observed in this study. Our results indicate that the healing of coherencies is affected only by a small crustal volume, whereas the surface deformations extend over a region of some 10 km. Nevertheless it is possible that the subsurface changes reported here also cause some of the surface deformation signal.

Our observations are interesting also in the light of the suggestion by *Revenaugh [1995]* that regions of high

scattering potential are characterized by enhanced seismicity (and earthquake slip). While he favors a structural (time independent) nature of the scatterer, the recovery process after the Loma Prieta earthquake suggests that some of this scattering may be due to fluid-filled cracks.

6. Conclusions

We inspected correlations and lapse time-dependent coherencies of several groups of similar events (multiplets) around the Loma Prieta rupture zone. Reduced coherency of post-Loma Prieta events with pre-Loma Prieta events occurred in a spatially limited region close to the Loma Prieta hypocenter. On the basis of multiple redundancy of the data set we were able to exclude contaminating effects, such as source variations, and to relate our observations to subsurface changes of seismic wave propagation properties. Successive combinations of the preshock and aftershocks, the latter sampling > 5 years of the postseismic period, revealed a progressive “healing” of these changes following approximately a power law dependence. The spatial pattern of temporally varying phases is best explained by local changes of scattering properties in the vicinity of the Loma Prieta source volume. To interpret these changes, we suggest a model of coseismically opened cracks acting as

seismic scatterers. Theoretical models of postseismic relaxation such as crack healing, fluid diffusion, and postevent deformation are possible explanations for the observed time signal.

Appendix A: Confidence Interval on the Coherency

In order to compute a confidence interval on the coherency $C(\nu)$ we follow *Got and Fréchet* [1993] using Fisher's z transformation

$$z = \frac{1}{2} \ln \frac{1 + C(\nu)}{1 - C(\nu)}, \quad (\text{A1})$$

where z is approximately Gaussian distributed with mean μ and variance $\sigma^2 = 1/(B_w T)$. Here B_w denotes the equivalent bandwidth of the smoothing function, and T is the sampling period. The 100(1- α)% lower and upper confidence interval for z is given by

$$\mu \pm \frac{\eta[1 - \alpha/2]}{\sqrt{B_w T}}. \quad (\text{A2})$$

For the assumed normal distribution, probability values of $\eta[1 - \alpha/2]$ can be derived from tabulated values [e.g., *Jenkins and Watts*, 1968, p.71]. After backtransformation, the 100(1- α)% confidence interval for the coherency is

$$I_c = \left[\tanh \left(z - \frac{\eta[1 - \alpha/2]}{\sqrt{B_w T}} \right), \tanh \left(z + \frac{\eta[1 - \alpha/2]}{\sqrt{B_w T}} \right) \right]. \quad (\text{A3})$$

Note that this confidence interval is not centered on $C(\nu)$.

Acknowledgments. All data used in this study are made available through the NCEDC and were contributed by the NCSN. We thank the staff of the USGS, Menlo Park, for providing information on instrument changes and Greg Beroza and David Schaff for valuable discussion and the compilation of the multiplet data sets. Constructive comments of Rick Aster and an anonymous reviewer are gratefully acknowledged.

References

- Aki, K., and B. Chouet, Origin of coda waves, attenuation, and scattering effects, *J. Geophys. Res.*, **80**(23), 3322-3342, 1975.
- Aki, K., T. DeFazio, P. Reasenberg, and A. Nur, An active experiment with earthquake fault for an estimation of the in situ stress, *Bull. Seismol. Soc. Am.*, **60**(4), 1315-1336, 1970.
- Antolik, M., R. M. Nadeau, R. C. Aster, and T. V. McEvelly, Differential analysis of coda Q using similar microearthquakes in seismic gaps, part 2, Application to seismograms recorded by the Parkfield High Resolution Seismic Network, *Bull. Seismol. Soc. Am.*, **86**(3), 890-910, 1996.
- Aster, R. C., P. M. Shearer, and J. Berger, Quantitative measurements of shear wave polarizations at the Anza seismic network, southern California: Implications for shear wave splitting and earthquake prediction, *J. Geophys. Res.*, **95**(B8), 12,449-12,473, 1990.
- Aster, R. C., G. Slad, J. Henton, and M. Antolik, Differential analysis of coda Q using similar microearthquakes in seismic gaps, part 1, Techniques and application to seismograms recorded in the Anza seismic gap, *Bull. Seismol. Soc. Am.*, **86**(3), 868-889, 1996.
- Beroza, G., Rupture history of the earthquake from high-frequency strong-motion data, in *The Loma Prieta, California, Earthquake of October 17, 1989-Main-Shock Characteristics*, edited by P. Spudich, *U.S. Geol. Surv., Prof. Pap.*, 1550-A, A9-A32, 1996.
- Beroza, G. C., A. T. Cole, and W. L. Ellsworth, Stability of coda wave attenuation during the Loma Prieta, California, earthquake sequence, *J. Geophys. Res.*, **100**(B3), 3977-3987, 1995.
- Beroza, G. C., D. Schaff, W. L. Ellsworth, A. T. Cole, and D. A. Dodge, Temporal changes in seismic velocities observed in the shear wave coda related to the 1989 Loma Prieta, California, earthquake, *Eos Trans. AGU*, **78**(46), Fall Meet. Suppl., F482, 1997.
- Bokelmann, G. H. R., and H.-P. Harjes, Evidence for temporal variation of seismic velocity within the upper continental crust, *J. Geophys. Res.*, **105**(B10), 23,879-23,894, 2000.
- Booker, J. R., Time dependent strain following faulting of a porous medium, *J. Geophys. Res.*, **79**(14), 2037-2044, 1974.
- Bürgmann, R., P. Segall, M. Lisowski, and J. Svarc, Post-seismic strain following the 1989 Loma Prieta earthquake from GPS and leveling measurements, *J. Geophys. Res.*, **102**(B3), 4933-4955, 1997.
- DeFazio, T. L., K. Aki, and J. Alba, Solid earth tide and observed change in the in situ seismic velocity, *J. Geophys. Res.*, **78**(8), 1319-1322, 1973.
- Dodge, D. A., and G. C. Beroza, Source array analysis of coda waves near the 1989 Loma Prieta, California, main-shock: Implications for the mechanism of coseismic velocity changes, *J. Geophys. Res.*, **102**(B11), 24,437-24,458, 1997.
- Eisler, J. D., Investigation of a method for determining stress accumulation at depth, *Bull. Seismol. Soc. Am.*, **57**(5), 891-911, 1967.
- Eisler, J. D., Investigation of a method for determining stress accumulation at depth-II, *Bull. Seismol. Soc. Am.*, **59**(5), 43-58, 1969.
- Ellsworth, W. L., A. T. Cole, G. C. Beroza, and M. C. Verwoerd, Changes in crustal wave velocity associated with the 1989 Loma Prieta, California, earthquake, *Eos Trans. AGU*, **73**(43), Fall Meet. Suppl., F360, 1992.
- Geller, R. J., and C. S. Mueller, Four similar earthquakes in central California, *Geophys. Res. Lett.*, **7**(10), 821-824, 1980.
- Got, J. L., and J. Fréchet, Origins of amplitude variations in seismic doublets: Source or attenuation process, *Geophys. J. Int.*, **114**, 325-340, 1993.
- Got, J. L., G. Poupinet, and J. Fréchet, Changes in source and site effects compared to coda Q^{-1} -Temporal variations using microearthquakes doublets in California, *Pure Appl. Geophys.*, **134**(2), 195-228, 1990.
- Hellweg, M., P. Spudich, J. B. Fletcher, and L. M. Baker, Stability of coda Q in the region of Parkfield, California: View from the U.S. Geological Survey Parkfield dense seismograph array, *J. Geophys. Res.*, **100**(B2), 2089-2102, 1995.
- Holzer, T. L., Extensive research on Loma Prieta improves understanding of earthquakes, *Eos Trans. AGU*, **80**(41), 482-483, 1999.
- Jack, I., Time-lapse seismic in reservoir management, paper presented at Society of Exploration Geophysicists, Tulsa, Okla., 1998.

- Jenkins, G. M., and D. G. Watts, *Spectral Analysis and Its Applications*, 525 pp., Holden-Day, Boca Raton, Fla., 1968.
- Kanamori, H., and G. Fuis, Variation of *P*-wave velocity before and after the Galway Lake earthquake ($M_L = 5.2$) and the Goat Mountain earthquakes ($M_L = 4.7, 4.7$) in the Mojave desert, California, *Bull. Seismol. Soc. Am.*, 66(6), 2017-2037, 1976.
- Karageorgi, E., R. Clymer, and T. V. McEvelly, Seismological studies at Parkfield, II, Search for temporal variations in wave propagations using vibroseis, *Bull. Seismol. Soc. Am.*, 82(3), 1388-1415, 1992.
- Leśniak, A., and H. Niituma, Time-frequency coherency analysis of three-component crosshole seismic data for arrival detection, *Geophysics*, 63(6), 1847-1857, 1998.
- Li, Y.-G., J. E. Vidale, K. Aki, F. Xu, and T. Burdette, Evidence of shallow fault zone strengthening after the 1992 $M7.7$ Landers, California, earthquake, *Science*, 279, 217-219, 1998.
- Neuhauser, D. S., B. Bogaert, and B. Romanowitz, Data access of northern California seismic data from the Northern California Earthquake Data Center, *Eos Trans. AGU*, 75(44), Fall Meet. Suppl., F429, 1994.
- Nur, A., and J. Walder, Hydraulic pulses in the Earth's crust, in *Fault Mechanics and Transport Properties of Rocks*, edited by B. Evans and T.-F. Wong, pp. 461-473, Academic, San Diego, Calif., 1992.
- Reasenber, P. A. (Ed.), The Loma Prieta, California, earthquake of October 17, 1989-Aftershocks and postseismic effects, *U.S. Geol. Surv. Prof. Pap.*, 1550-D, 1997.
- Revenaugh, J., Relation of the 1992 Landers, California, earthquake sequence to seismic scattering, *Science*, 270, 1344-1347, 1995.
- Sato, H., Temporal change in scattering and attenuation associated with the earthquake occurrence-A review of recent studies on coda waves, *Pure Appl. Geophys.*, 126(2-4), 465-497, 1988.
- Savage, J. C., M. Lisowski, and J. L. Svarc, Postseismic deformation following the 1989 ($M=7.1$) Loma Prieta, California, earthquake, *J. Geophys. Res.*, 99(B7), 13,757-13,765, 1994.
- Schaff, D., G. C. Beroza, and B. E. Shaw, Postseismic response of repeating aftershocks, *Geophys. Res. Lett.*, 25(24), 4549-4552, 1998.
- Segall, P., R. Bürgmann, and M. Matthews, Time-dependent triggered afterslip following the 1989 Loma Prieta earthquake, *J. Geophys. Res.*, 105(B3), 5615-5634, 2000.
- Simpson, R. W. (Ed.), The Loma Prieta, California, earthquake of October 17, 1989-Tectonic processes and models, *U.S. Geol. Surv. Prof. Pap.*, 1550-F, 1994.
- Smith, D. L., and B. Evans, Diffusional crack healing in quartz, *J. Geophys. Res.*, 89(B6), 4125-4135, 1984.
- Spudich, P. (Ed.), The Loma Prieta, California, earthquake of October 17, 1989-Main-shock characteristics, *U.S. Geol. Surv. Prof. Pap.*, 1550-A, 1996.
- Wesson, R. L., R. Robinson, C. G. Bufe, W. L. Ellsworth, J. H. Pfluke, J. A. Steppe, and L. C. Seekins, Search for seismic forerunners to earthquakes in central California, *Tectonophysics*, 42, 111-126, 1977.

S. Baisch, Ruhr-Universität Bochum, Institut für Geophysik, Universitätsstrasse 150, D-44780 Bochum, Germany. (baisch@geophysik.ruhr-uni-bochum.de)

G. H. R. Bokelmann, Department of Geophysics, Stanford University, Stanford, CA 94305-2215. (goetz@pangea.stanford.edu)

(Received June 1, 2000; revised January 11, 2001; accepted March 13, 2001.)